

Q C D string in light-light and heavy-light m esons

Yu S K alashnikova ^a, A V Nefediev ^{a,b}, Yu A Sim onov ^a

^a Institute of Theoretical and Experimental Physics, 117218,

B C herem ushkinskaya 25, M oscow, Russia

^bCentro de F sica das Interacões Fundamentais (C F IF), D epartamento de F sica,

I nstituto Superior T ecnico, A v. Rovisco P ais, P -1049-001 L isboa, P ortugal

A bstract

Spectra of light-light and heavy-light m esons are calculated within the framework of the Q C D string m odel, which is derived from Q C D in the W ilson loop approach. Special attention is payed to the proper string dynamics that allows to reproduce the straight-line Regge trajectories with the inverse slope being 2 for light-light and as twice as smaller for heavy-light m esons.

We use the m odel of the rotating Q C D string with quarks at the ends to calculate m asses of several light-light m esons lying on the lowest Regge trajectories and compare them with the experimental data as well as with the predictions of other m odels.

M asses of several low-lying orbitally and radially excited heavy-light states in the D , D _s, B and B _s m esons spectra have been calculated in the einbein (auxiliary) eld approach, which is proven to be rather accurate in various calculations for relativistic systems. The results for the spectra have been compared with the experimental and recent lattice data. It is demonstrated that the account for the proper string dynamics encoded in the so-called string correction to the interquark interaction leads to extra negative contribution to the m asses of orbitally excited states that resolves the problem of identification of the D (2637) state recently claimed by D E L P H I C ollaboration.

For the heavy-light system we extract the constants α_1 and α_2 used in the Heavy Quark Effective Theory (HQET) and find a good agreement with the results of other approaches.

PACS: 12.38Aw, 12.39Hg, 12.39Ki

I. INTRODUCTION

Description of the mass spectrum of hadrons is one of the fundamental problems of strong interactions. It has been attacked in a sequence of approaches motivated by QCD, but still attracts considerable attention. One of the most intriguing phenomena, namely the formation of an extended object, the QCD string, between the colour constituents inside hadrons, plays a crucial role in understanding their properties. In the present paper this role is exemplified by spectra of mass of light-light and heavy-light mesons. In the former case we study the role played by the QCD string in formation of the straight-line Regge trajectories and discuss the form of the interquark interaction inside light hadrons. For heavy-light mesons we find the masses of several low-lying states in the D , D_s , B and B_s mesons spectra including orbitally and radially excited ones.

We calculate and discuss the spin-spin and spin-orbit splittings and compare them to the experimental and recent lattice data. A special attention is payed to the role of the proper string dynamics in establishing the correct slope of the Regge trajectories for both, light-light and heavy-light states, as opposed to those following from the relativistic equations with local potentials.

We remind then that an extra piece of the effective interquark potential, the string correction, which is entirely due to the string-type interaction in QCD [1,2], gives negative contribution into the masses of orbitally excited states. The latter observation allows to resolve the "mystery" of an extremely narrow $D(2637)$ state (and similar one in the B -mesonic spectrum) [3] recently claimed by DELPHI collaboration [4,5]. We present a reasonable

for the several lowest states in D – and B – mesonic spectra using the standard values for the string tension, the strong coupling constant and the current quark masses. We also find the correspondence between our model and the Heavy Quark Effective Theory extracting the constants used in the latter approach in the expansion of a heavy–light meson mass in the inverse powers of the heavy quark mass. We find analytical formulae for these constants and compare their numerical estimates with the predictions of other models.

The two main approaches used in the numerical calculations are the quasiclassical method of solving the eigenenergies problem and the variational one based on the einbein field formalism. Accuracy of both methods is tested using exactly solvable equations and found to be about 7% at worst even for the lowest states. Possible improvements of the method are outlined and discussed.

The paper is organized as follows. In Section II we give a brief insight into various aspects of the einbein field formalism. In Section III the exact spectra of relativistic equations are confronted to the results of approximate calculations using the quasiclassical and variational einbein field methods, as well as the combined one. In Section IV we discuss the problem of the Regge trajectories slopes as they appear from the relativistic equations with local potentials and from the string-like picture of confinement. Derivation of the Hamiltonian for the spinless quark-antiquark system as well as of the spin-dependent corrections to it is the subject of Section V. Spectra of light-light and heavy-light mesonic states are calculated and discussed in Sections VI and VII respectively. Section VIII contains our conclusions and outlook.

II. EINBEIN FIELD FORMALISM

In this section we give a short introduction into the method of the einbein fields and its possible applications to relativistic systems. An interested reader can find a more detailed information in [6] and references therein.

A . R eparametrization invariance and constrained systems

Historically einbein field formalism was introduced in [7] to treat the kinematics of the relativistic spinless particles. Later it was generalized for the case of spinning particles [8] and strings [9]. So, the action of a free relativistic particle can be rewritten as¹

$$S = \int_{i}^{f} L(\dot{x}); \quad L = m \frac{p \underline{x}^2}{2} - \frac{m^2}{2}; \quad (1)$$

where the dot denotes derivative with respect to the proper time τ , \dot{x} being the einbein field². The original form of the action can be easily restored after solving the Euler-Lagrange equation of motion for the einbein which amounts to taking extremum in the latter. Note that the invariance of the initial action with respect to the change of the proper time

$$! f(\tau) \frac{df}{d\tau} > 0 \quad f(\tau_i) = \tau_i \quad f(\tau_f) = \tau_f \quad (2)$$

is preserved if an appropriate re-scaling is prescribed to \dot{x} :

$$! \dot{x} = f \dot{\tau} \quad (3)$$

The latter invariance means that one deals with a constrained system. For the free particle the only constraint defines the mass shell

$$p^2 - m^2 = 0; \quad (4)$$

or in presence of the einbein field

$$= 0 \quad H = \frac{p^2 - m^2}{2}; \quad (5)$$

¹In the path integral formalism this transformation is based on the following relation

$$Z = \int D(\tau) \exp \left(- \int d\tau \left(\frac{a}{2} \dot{x}^2 + \frac{b}{2} \dot{p}^2 \right) \right) \exp \left(- \int d\tau \frac{p \underline{x}}{ab} \right);$$

²Usually $e = \frac{1}{\dot{x}}$ is referred as the einbein [7].

with \dot{q} being the momentum canonically conjugated to q , H is the Hamiltonian function of the system (in case (4) it identically vanishes). Requirement that the constraint $\dot{q} = 0$ is preserved in time returns one to the mass-shell condition (4):

$$0 = \dot{q} = f \cdot H \cdot g = \frac{\partial H}{\partial \dot{q}} = \frac{p^2 - m^2}{2} - p^2 = m^2: \quad (6)$$

To make things simpler, one can fix the gauge-like freedom (2) identifying the proper time τ with one of the physical coordinates of the particle. The most popular choices are the laboratory gauge ($\tau = q$);

the proper time gauge ($\tau = (nx)$, $n = \frac{p^2}{P^2}$ with P being the total momentum of the system) [10];

the light-cone gauge ($\tau = \frac{1}{2}(x_0 + x_3) = x_+$),

which lead to quantization of the system on different hypersurfaces.

With the laboratory gauge fixed the Lagrangian function (1) becomes

$$L = \frac{m^2}{2} - \frac{\dot{q}^2}{2} + \frac{\dot{x}^2}{2}; \quad (7)$$

so that the corresponding Hamiltonian function reads

$$H = \frac{p^2 + m^2}{2} + \frac{\dot{x}^2}{2}; \quad (8)$$

and after taking extremum in τ one ends with the standard relativistic expression

$$H = \frac{q^2}{p^2 + m^2}; \quad (9)$$

B. Einbeins as variational parameters

In the simple example considered above neither the Lagrange, nor the Hamilton functions of the system contained \dot{q} that allowed to get rid of \dot{q} at any stage by taking extremum in the latter. It is not so for more complicated systems when a change of variables is to

be performed which touches upon the einbeins. The velocity corresponding to the original degrees of freedom of the system may mix in a very tangled way with those for einbeins, so that it is not a simple task anymore to follow the lines à la Dirac [11] to resolve the set of constraints and to get rid of non-physical degrees of freedom. See e.g.: [6,8,12] for several examples when such a resolution can be done explicitly.

Luckily another approach to einbeins is known [2,13]. They can be treated as variational parameters. Thus one replaces the dynamical function of time (τ) by the parameter τ_0 independent on τ . The eigenstates problem is solved then keeping τ_0 constant, so that one has the spectrum $M_{\text{fng}}(\tau_0)$, where fng denotes the full set of quantum numbers. Then one is to minimize each eigenenergy independently with respect to τ_0 ³:

$$\frac{\partial M_{\text{fng}}(\tau_0)}{\partial \tau_0} = 0 \quad M_{\text{fng}} = M_{\text{fng}}(\tau_0); \quad (10)$$

Such an approach has a number of advantages. First, it allows to avoid tedious algebra of commuting constraints with one another following the standard Dirac technique [11]. Second, it allows a very simple and physically transparent interpretation of einbeins. Indeed, in formulae (1) and (7) the einbein ϵ can be treated as an effective mass of the particle; dynamics of the system remains essentially relativistic, though being non-relativistic in form. If m is the current quark mass, then ϵ can be viewed as its constituent mass celebrated in hadronic phenomenology. What is more, the current mass can be even put to zero, whereas the Lagrangian approach remains valid in presence of the einbeins and the standard Hamiltonian technique can be developed then. The latter observation is intensively used in the analytic QCD calculations for glue describing gluonic degrees of freedom in glueballs and hybrids [14,15].

³Note that solutions for τ_0 of both signs appear, but only one of them ($\tau_0 > 0$) is really left. Neglecting the negative solution is the general lack of the einbein field approach and this leads to the fact that quark Zitterbewegung is not taken into account (see also discussion in Subsection III D).

An obvious disadvantage of the variational approach to the einbein fields is some loss of accuracy. As a variational method it provides only an approximate solution giving no hint on how to estimate the ultimate accuracy of the results. Thus in the next section we test this method comparing its predictions with the exact solutions of some relativistic equations. We consider the accuracy, found to be about 7% at worst, quite reasonable, that justifies our consequent attack at the light-light and heavy-light mesons spectra using this formalism.

III. TEST IN G THE METHOD

A. Quasiclassics for the spinless Salpeter equation

We start from the Salpeter equation for the quark-antiquark system with equal masses and restrict ourselves to the zero angular momentum case for simplicity:

$$\frac{q}{2} \frac{1}{p_r^2 + m^2} + r_n = M_n^{(11)} n; \quad (11)$$

where the subscript (11) stands for the light-light system.

The quasiclassical quantization condition looks like

$$\int_0^{r_+} p_r(r) dr = n + \frac{3}{4}; \quad n = 0, 1, 2, \dots; \quad r_+ = \frac{M_n^{(11)} - 2m}{2m}; \quad (12)$$

where the integral on the l.h.s. can be worked out analytically yielding

$$M_n^{(11)} \frac{r}{M_n^{(11)} - 2m} - \frac{4m^2}{4m^2 \ln \frac{M_n^{(11)} - 2m}{2m}} = n + \frac{3}{4}; \quad (13)$$

or approximately (in $m \ll p$) one has

$$M_n^{(11)} = 4n + \frac{3}{4} + 2m^2 \ln \frac{(n + 3/4)}{m^2} + \dots \quad (14)$$

Solution (14) becomes exact in the limit $m = 0$, whereas for a nonzero mass the leading correction to the linear regime $(M_n^{(11)})^2$ in n behaves like

$$\frac{M_n^{(11)} - 2m}{M_n^{(11)} + 2m} = O\left(\frac{m^2}{M_n^{(11)} + 2m} \ln \frac{M_n^{(11)} - 2m}{m^2}\right) \stackrel{!}{=} n + \frac{\ln n}{n}; \quad (15)$$

For a heavy-light system one has the Salpeter equation

$$q \frac{1}{p_r^2 + m^2} + r_n = M_n^{(h)} n; \quad (16)$$

where $M_n^{(h)}$ denotes the excess over the heavy particle mass M . Similarly to (13) one finds then

$$\frac{r}{M_n^{(h)} - M_n^{(h)} \frac{2}{m^2}} = \frac{r}{m^2 \ln \frac{M_n^{(h)} \frac{2}{m^2} + M_n^{(h)}}{m}} = 2 n + \frac{3}{4}; \quad (17)$$

and the formula (15) holds true in this case as well.

Comparing the results of the WKB method with the exact solutions of the equation (11) (raws M_n (WKB) and M_n (exact) in Table I), one can see that the error does not exceed 3-4% even for the ground state. See also [16] where the WKB method is tested for light-light mesons.

B. Quasiclassics for the one-particle Dirac equation

As a next example we discuss the one-particle Dirac equation with linearly rising conning potential [17]:

$$(\not{p} + (m + U) + V) n = " n; \quad (18)$$

The WKB method applied to this equation gives [18,19]

$$\int_{r_+}^r p + \frac{w}{pr} dr = n + \frac{1}{2}; \quad n = 0, 1, 2, \dots; \quad (19)$$

where

$$p = (\not{m} - V)^{\frac{1}{2}} \frac{1}{r^2} (\not{m} + U)^{\frac{1}{2}}; \quad (20)$$

$$w = \frac{1}{2r} \frac{1}{2m + U + "} \frac{U^0 - V^0}{V};$$

$$j \rightarrow j + \frac{1}{2};$$

For the most interesting case of purely scalar component ($V = 0, U = -r$) an approximate quasiclassical solution was found in [19] ($m = 0$):

$$\frac{m^2}{n} = 2 \cdot 2n + j + \frac{3}{2} + \frac{\text{sgn}}{2} + \frac{!}{\frac{m^2}{n}} \cdot 0.38 + \ln \frac{\frac{m^2}{n}}{j} + O \cdot \frac{!}{\frac{m^2}{n}} \cdot A^A : \quad (21)$$

Detailed comparison of the results of the WKB method and those following from the recursive formula (21) with the exact numerical solutions to equation (18) is given in [20]. Here we only note that the coincidence of the three numbers is impressive as even for the lowest states the discrepancy does not exceed 1%.

C. Quasiclassical variational einbein field (combined) method for the spinless

Salpeter equation

Finally we combine the two methods discussed above and apply the WKB approximation to the Hamiltonian of a relativistic system with einbeins introduced as variational parameters. Then the resulting quasiclassical spectrum is minimized with respect to the einbeins. Thus we have a powerful method of solving the eigenvalues problem for various relativistic systems which we call "combined". Let us test the accuracy of this method first.

We start from the Salpeter equation (11) for the light-light system and introduce the parameter α as described in Section II:

$$H_1 = 2 \cdot \frac{q}{p_r^2 + m^2 + r} \cdot ! \quad H_2 = \frac{p_r^2 + m^2}{\alpha} + \alpha + r: \quad (22)$$

In what follows we consider the massless case substituting $m = 0$ into (22).

We give the analytic formulae for the spectrum of the Salpeter equation (11) obtained using the quasiclassical approximation for the Hamiltonian H_1 (following from equation (13) for $m = 0$), the exact solution for the Hamiltonian H_2 minimized with respect to the einbein field and the result of the combined method when the Bohr-Sommerfeld quantization condition is applied to the Hamiltonian H_2 and the ultimate spectrum is also minimized with respect to α .

$$M_n^2 (WKB) = 4 \quad n + \frac{3}{4} \quad (23)$$

$$M_n^2 (\text{einbein}) = 16 \quad \frac{n+1}{3} \quad !_{3=2} \quad (24)$$

$$M_n^2 (\text{combined}) = \frac{8}{p=3} \quad n + \frac{3}{4} ; \quad (25)$$

where $n+1$ is the $(n+1)$ -th zero of the Airy function $Ai(z)$ and counting of zeros starts from unity. The extremal values of the einbein field in the latter two cases read

$$_0 (\text{einbein}) = p - \frac{n+1}{3} \quad !_{3=4} \quad _0 (\text{combined}) = \frac{v}{t} \frac{(n+3=4)}{2 \frac{p}{3}} ; \quad (26)$$

i.e. the effective quark mass is $_0 p -$ and it appears entirely due to the interquark interaction.

In Table I we compare the results of the above three approximate methods of solving the eigenvalues problem for equation (11) with the exact solution. In the last raw we give the accuracy of the combined method vs the exact solution. Two conclusions can be deduced from Table I. The first one is that the accuracy of all approximate methods is high enough, including the combined method which is of most interest for us in view of its consequent applications to the QCD string with quarks at the ends. The other conclusion is that the variational einbein field method gives a systematic overestimation for the excited states which is of order 5-7%.

D . D discussion

Here we would like to make a couple of concluding comments concerning the numerical methods tested in this section, their accuracy and possible ways of its improvement. As stated above the combined quasiclassical variational method is of most interest for us, so we shall concentrate basically on it. The following two remarks are in order here.

From Table I one can see that the relative error is practically constant tending to the value of 7% for large n . The reason for such a behavior will become clear if one compares formulae

(23) and (25). Both relations reproduce the same dependence on the radial quantum number n , whereas the difference comes from different slopes, 4 in (23) vs $\frac{8}{3}$ in (25). Then for highly excited states the error is practically independent on n and can be estimated as

$$= \frac{M_n(\text{combined}) - M_n(\text{exact})}{M_n(\text{combined})} \quad \frac{M_n(\text{combined}) - M_n(\text{WKB})}{M_n(\text{combined})} = 1 - \frac{\frac{8}{3} - 4}{2} = 0.07; \quad (27)$$

i.e. the ultimate accuracy of the quasiclassical variational einbein field method (combined method) appears to be about 7%. Introducing, say, a correcting factor in (25) one could overcome the systematic overestimation and reproduce the spectrum with a better accuracy. We shall return to this observation later on when discussing the spectrum of the heavy-light mesons.

Another source of the error in the einbein field approach is neglecting the quark Zitterbewegung (see the footnote on page 6). As stated above we neglect the negative sign solution for the einbein field ϵ_0 expecting its small influence on the spectrum. Let us give some reasonings to justify this action.

It was demonstrated numerically in [21] that the contribution of the quark Z-graphs into M^2 is nearly constant for large excitation numbers and is of order of 10%, so that the corresponding shift of M behaves like

$$M \approx \frac{M^2}{M} \approx \frac{1}{n-1} \frac{1}{\frac{8}{3}}; \quad (28)$$

so it is somewhat suppressed.

Besides, a good agreement of our numerical results with those provided by the lattice data and taken from the Particle Data Group can also serve as an a posteriori justification of such neglecting. Still some improvements for the einbein field approach are needed to take this effect into account.

IV . REGGE TRAJECTORIES FOR RELATIVISTIC EQUATIONS WITH LOCAL
POTENTIALS

It was observed long ago that the mesonic Regge trajectories are almost linear if the total momentum or the radial quantum number are plotted vs the mesonic mass squared [22]:

$$M^2(n;J) = c_n n + c_J J + M^2; \quad (29)$$

where c_n and c_J are the (inverse) slopes while M^2 denotes corrections to the leading linear regime which come from the self energy, spin splittings etc.

Relations like (29) naturally appear in most of models for constituent, though the (inverse) slopes c_n and c_J are different for different models.

For example Salpeter equation for the heavy-light system

$$\frac{q}{p_r^2 + p_{r'}^2 + m^2 + r_{nl}} = M_{nl}; \quad (30)$$

gives

$$c_J^{(h1)}(\text{Salpeter}) = 4; \quad c_n^{(h1)}(\text{Salpeter}) = 2; \quad (31)$$

where the total momentum J coincides with the orbital one l .

For the light-light system one easily finds from (31) by a trivial parameters re-scaling:

$$c_J^{(ll)}(\text{Salpeter}) = 8; \quad c_n^{(ll)}(\text{Salpeter}) = 4; \quad (32)$$

One-particle Dirac equation (18) yields different slopes for different natures of the connecting force. Thus for the purely vector constituent (potential added to the energy term ⁴) one finds

$$c_J^{(h1)}(\text{Dirac}) = 4; \quad (33)$$

whereas for purely scalar constituent (potential added to the mass term)

⁴We disregard the problem of the Klein paradox here.

$$c_J^{(h1)}(D_{\text{irac}}) = 2 : \quad (34)$$

In the meantime the spectrum (29) is expected to follow from a string-like picture of confinement which predicts the (inverse) Regge slopes to be

$$c_J^{(11)}(\text{string}) = 2 \quad c_J^{(h1)}(\text{string}) = \quad : \quad (35)$$

One can easily see that none of the relativistic equations considered before gives the correct result (35), moreover the discrepancies are rather large (of order 25%). See also [23] for discussion of various models of confinement and the corresponding Regge trajectories slopes.

The reason why relativistic Salpeter and Dirac equations fail to reproduce the correct string slope of the Regge trajectories is obvious and quite physically transparent. Indeed, all relativistic equations with local potentials have only trivial dependence of the interquark interaction on the angular momentum which comes entirely from the quark kinetic energy. Meanwhile QCD is believed to lead to a string-type interaction between the colour constituents inside hadrons, whereas the QCD string developed between quarks possesses its own inertia and thus it should also contribute to the J -dependent part of the interaction. It is this extra purely string-type piece of the interquark interaction to give extra contribution into the Regge trajectories slope and to bring it into the correct form of (35). This statement is proven explicitly in the next section, whereas the string dynamics footprint in the heavy-light mesons spectrum is discussed in detail in Section V II.

V. HAMILTONIAN OF THE QQ MESON

A. Quark-antiquark Green's function

We start from the Euclidean Green's function of the $q\bar{q}$ pair in the confining vacuum

$$G_{q\bar{q}} = h_{q\bar{q}}^{(f)}(x; y) \hat{A}^+ - h_{q\bar{q}}^{(i)}(x; y) \hat{A}^- i_{q\bar{q}\bar{A}} ; \quad (36)$$

where the initial and the final mesonic wave functions

$$\frac{(i,f)}{q\bar{q}}(x;y) = \frac{1}{q(x)}(x;y) \frac{(i,f)}{q(y)} \quad (37)$$

are gauge invariant due to the standard path-ordered parallel transporter

$$(x;y) = P \exp \left[ig \int_y^x dz A \right]; \quad (38)$$

(i,f) denote the matrices which might be inserted into the initial and final meson-quark-antiquark vertices.

Integrating out the quark fields in (36), one finds for the mesonic Green's function

$$G_{qq} = hT r^{(f)} S_q(x;x) (x;y) \frac{(i)}{S_q(y;y)} (y;x) i_A; \quad (39)$$

where the trace stands for both, colour and spinor indices. We have neglected here the $1=N_C$ suppressed quark determinant, describing sea quark pairs.

To proceed further we employ the Feynman-Schwinger representation for the one-fermion propagators in the external field, x the laboratory gauge for both particles

$$x_{10} = t_1 \quad x_{20} = t_2 \quad (40)$$

and introduce the einbein fields ϵ_1 and ϵ_2 by means of the following change of variables (see [24,2] for details)

$$\epsilon_i(t_i) = \frac{T}{2s_i} x_{i0}(t_i) \quad ds_i D x_{i0} \quad ! \quad D \epsilon_i(t_i) \quad i=1,2; \quad (41)$$

where $s_{1,2}$ are the Schwinger times, $T = \frac{1}{2}(x_0 + x_0 - y - y)$.

Then the resulting expression for the mesonic Green's function reads [24]

$$G_{qq} = \int_0^T D \epsilon_1(t_1) D \epsilon_2(t_2) D x_1 D x_2 e^{-K_1 - K_2} T r^{(f)} (m_1 \hat{D})^{(i)} (m_2 \hat{D}) \quad (42)$$

$$P \exp \left[\int_0^T \frac{dt_1}{2 \epsilon_1(t_1)} \frac{(1)}{i s(x_1(t_1))} \exp \left[\int_0^T \frac{dt_2}{2 \epsilon_2(t_2)} \frac{(2)}{i s(x_2(t_2))} \exp \left(- \frac{1}{2} \int_0^T dt_2 \epsilon_2^2(t_2) \right) \right] \right] \quad (43)$$

with K_i being the kinetic energies of the quarks

$$K_i = \int_0^T dt_i \left(\frac{m_i^2}{2} + \frac{i \epsilon_i}{2} + \frac{i \epsilon_i^2}{2} A \right); \quad i=1,2; \quad (44)$$

$= \frac{1}{4i} (\dots)$ and $= s$ denotes the derivative with respect to the element of the area S . We have also used the minimal area law asymptotic for the isolated Wilson loop

$$Tr P \exp \left[ig \int_C^A dz A \right] \exp(-S_{min}); \quad (44)$$

which is usually assumed for the stochastic QCD vacuum (see e.g. [25]) and found on the lattice. Here S_{min} being the area of the minimal surface swept by the quark and the antiquark trajectories.

Looking at (42) one can easily recognize the following three main ingredients: the contribution of the quark, the one of the antiquark and finally the connecting interaction given by the string with tension σ . One can write for the latter

$$S_{min} = \int_0^{Z_T} dt \int_0^{Z_1} d\zeta \frac{q}{(w_w^0)^2 - w^2 w^0}; \quad (45)$$

with $w(t; \zeta)$ being the string profile function chosen in the linear form

$$w(t; \zeta) = x_1(t) + (1 - x_1) \zeta; \quad (46)$$

thus describing the straight-line string which is a reasonable approximation for the minimal surface [2].

Finally, synchronizing the quark and the antiquark times ($t_1 = t_2 = t$) one finds from (42) that in the spinless approximation the quark-antiquark meson can be described by the Lagrangian

$$L(t) = \frac{m_1^2}{2} \frac{m_2^2}{2} - \frac{x_1^2 + x_2^2}{2} - \frac{x_1^2}{2} - \frac{x_2^2}{2} - \frac{q}{r} \int_0^{Z_1} d\zeta \frac{1}{1 + \frac{q}{r} (x_1 + (1 - x_1))^2}; \quad (47)$$

where $r = x_1 - x_2$ and $n = r = r$. Expansion of the surface-ordered exponents in (42) gives a set of spin-dependent corrections to the leading regime (47).

B. Hamiltonian for spinless quarks

Starting from the Lagrangian (47) and introducing an extra einbein field $(t; \zeta)$ continuously depending on the internal string coordinate one can get rid of the square root

in (47) arriving at the Hamiltonian of the qq system in the centre-of-mass frame in the form

[2]

$$\begin{aligned}
 H = \sum_{i=1}^{x^2} \frac{p_r^2 + m_i^2}{2} + \frac{!}{2} + \frac{z_1}{d} - \frac{r^2}{2} + \frac{!}{2} + \frac{\mathbf{L}^2}{2r^2 [(1 - \frac{!}{2})^2 + \frac{R_1^2}{d} (1 - \frac{!}{2})^2]}; \\
 = \frac{\frac{R_1}{d}}{1 + \frac{!}{2} + \frac{R_1}{d}};
 \end{aligned} \tag{48}$$

Similarly to 's which have the meaning of the constituent quark masses, the einbein can be viewed as the density of the string energy. In the simplest case of $l = 0$ one easily finds for the extremal value of

$$_0 = r; \tag{49}$$

i.e.: the energy distribution is uniform and the resulting interquark interaction is just the linearly rising potential r . In the meantime if $l \neq 0$ then the two contributions can be identified in the last l -dependent term in (48). Roughly speaking the first two l -dependent terms in the denominator come from the quark kinetic energy. The last term containing the integral over r is nothing but the extra inertia of the string discussed before. Rotating string also contributes to the interquark interaction making it essentially non-local, so that the very notion of the interquark potential is not applicable to the system anymore.

Note that the Hamiltonian (48) has the form of sum of the "kinetic" and the "potential" parts, but this is somewhat misleading, as extreme in all three einbeins are understood, so that the ultimate form of the Hamiltonian would be extremely complicated and hardly available for further analytical studies.

Expression (48) can be simplified if one expands the Hamiltonian in powers of $\frac{p}{r} = l$. One finds then [2,3]

$$H = H_0 + V_{\text{string}} \tag{50}$$

$$H_0 = \sum_{i=1}^{x^2} \frac{p_r^2 + m_i^2}{2} + \frac{!}{2} + r; \tag{51}$$

$$V_{\text{string}} = \frac{\left(\begin{smallmatrix} 2 & 2 & 1 & 2 \\ 1 & 2 & 1 & 2 \end{smallmatrix}\right) \frac{L^2}{r}}{6 \begin{smallmatrix} 2 & 2 \\ 1 & 2 \end{smallmatrix}}; \quad (52)$$

where V_{string} is known as the string correction [1,2] and this is the term totally missing in the relativistic equations with local potentials. Indeed, the Salpeter equation with the linearly rising potential is readily reproduced from (51) if extreme values in $\lambda_{1,2}$ are taken explicitly, whereas the string correction is lost. Meanwhile its sign is negative so that the contribution of the string lowers down the energy of the system thus giving negative contribution to the masses of orbitally excited states leaving those with $l=0$ intact. In Section VI we shall demonstrate how the proper account for the string dynamics in the full Hamiltonian (48) brings the Regge trajectories slope into the correct value (35), whereas in Section VII the string correction (52) will be demonstrated to solve the problem of the identification of the resonance D (2637) recently claimed by DELPHIC collaboration [4,5].

C. Spin-dependent corrections

Let us return to the quark-antiquark Green's function (42) and extract the nonperturbative spin-orbit interaction. Following [26,27] one finds

$$V_{\text{so}}^{\text{np}} = \frac{0}{2r} @ \frac{S_1 L}{\begin{smallmatrix} 2 \\ 1 \end{smallmatrix}} + \frac{S_2 L}{\begin{smallmatrix} 2 \\ 2 \end{smallmatrix}} A : \quad (53)$$

It follows from [26,27] that all potentials $V_i(r)$ (in the notations of [28]) contain both, perturbative and nonperturbative pieces given there in the explicit form. One can argue that at large distances the only piece (53) is left whereas for light quarks all nonperturbative ones may be important (see [29]).

Now, to have the full picture of the interquark interaction one is to supply the purely nonperturbative string-type interaction described by the Hamiltonian (48) by the perturbative gluon exchange adding the colour Coulomb potential to the Hamiltonian H_0 from (51) and calculating the corresponding spin-dependent perturbative terms in addition to the potential (53). The result reads

$$H_0 = \sum_{i=1}^{x^2} \frac{p_i^2 + m_i^2}{2} + \frac{r^i}{2} + r \frac{4s}{3r} C_0; \quad (54)$$

where we have also added the overall constant shift C_0 and

$$V_{sd} = \frac{8}{3} \begin{pmatrix} 1 & 2 \\ 1 & 2 \end{pmatrix} (S_1 S_2) \begin{pmatrix} 0 \\ 1 \end{pmatrix} \frac{1}{2r} \left[\frac{S_1 \tilde{L}}{2} + \frac{S_2 \tilde{L}}{2} A + \frac{1}{r^3} \begin{pmatrix} 1 & 0 \\ 2 & 1 \end{pmatrix} + \frac{1}{2} \begin{pmatrix} 1 & 0 \\ 2 & 1 \end{pmatrix} \frac{S_1 \tilde{L}}{1} + \frac{1}{r^3} \begin{pmatrix} 1 & 0 \\ 2 & 1 \end{pmatrix} \frac{S_2 \tilde{L}}{2} \right] + \frac{3}{r^3} (S_1 n) (S_2 n) \begin{pmatrix} 0 \\ 2 \end{pmatrix} + \frac{3}{2r^3} S \tilde{L} \begin{pmatrix} 2 & \ln(r) \end{pmatrix}; \quad n = 0.57; \quad (55)$$

with $\gamma = \frac{4}{3} s$, $\gamma = \frac{1-2}{1+2}$. We have also added the term of order $\frac{2}{s}$ which comes from one-loop calculations and is intensively discussed in literature [30,31,29]. It is important to stress that C_0 is due to the nonperturbative self-energy of light quarks, which explains the later numerical inputs.

An important comment concerning the expansion (55) is in order. Up to the last term the expression (55) coincides in form with the Eichten-Feiberg-Gromes result [28], but we have effective quark masses m_i in the denominators instead of the current ones $m_{i'}$. Once $\frac{q}{m_i^2} \frac{1}{h p^2 i + m_i^2} > m_i$ or even $m_i > m_{i'}$ then the result (55) is applicable to the case of light quark flavours, when the expansion of the interaction in the inverse powers of the quark mass m_i obviously fails. The values of m_i 's are defined dynamically and differ from state to state (see [26] for details).

The Hamiltonian (54) with spin-dependent terms (55) will be used for explicit calculations for heavy-light mesons. In case of light-light states one should include additional nonperturbative spin-dependent terms (see [26] and references therein). The masses of light-light mesons listed in Table II have been calculated from the Regge trajectories which do not take into account spin-dependent terms and we give them for the sake of comparison. A more detailed calculation for the light mesons taking these effects into account can be found in [29].

VI. SPECTRUM OF LIGHT-LIGHT MESONS

A . Angular momentum dependent potential and Regge trajectories

Starting from the Hamiltonian (48) we stick with the case of equal quark masses m

$$H = \frac{p_r^2 + m^2}{r} + \frac{L^2 = r^2}{+ 2R_0^1 \left(-\frac{1}{2} \right)^2 d} + \frac{z_1^2 r^2}{2} \frac{d}{z_1} + \frac{z_1^2}{2} d : \quad (56)$$

The extremal value of the einbein field can be found explicitly and reads [20]

$$_0(\lambda) = \sqrt{\frac{r}{1 - 4y^2 \left(-\frac{1}{2} \right)^2}}; \quad (57)$$

where y is the solution to the transcendental equation

$$\frac{L}{r^2} = \frac{1}{4y^2} (\arcsin y - y \sqrt{1 - y^2}) + \frac{y}{r}; \quad (58)$$

and $L^2 = 1(1+1)$.

For large angular momenta the contribution of the quarks (the last term on the r.h.s. of (58)) is negligible so that the maximal possible value $y = 1$ is reached, thus yielding the solution for the free open string [2] (see also the second entry in [12]).

With the extremal value $_0$ from (57) inserted, Hamiltonian (56) takes the form

$$H = \frac{p_r^2 + m^2}{(\lambda)} + (\lambda) + \frac{r}{y} \arcsin y + (\lambda) y^2 \quad (59)$$

with y defined by equation (58). The last two terms on the r.h.s. of equation (59) can be considered as an effective "potential"

$$U(\lambda; r) = \frac{r}{y} \arcsin y + (\lambda) y^2; \quad (60)$$

which is nontrivially λ -dependent. In Fig.1 we give the form of the effective potential (60) for a couple of low-lying states (solid line). It has the same asymptotic as the naive sum of the linearly rising potential and the centrifugal barrier coming from the kinetic energy of the quarks (dotted line). In the meantime it differs from the latter at finite distances. The only exception is the case of zero angular momentum which should be treated separately and leads to the linearly rising potential for any interquark separation.

B. Numerical results

Following the variational einbein field method described and tested above, we start from the Hamiltonian (59) and change the einbein field for the variational parameter α_0 [20], so that one has

$$H = \frac{p_r^2 + m^2}{\alpha_0} + \alpha_0 + U(\alpha_0; r) \quad (61)$$

$$U(\alpha_0; r) = \frac{r}{y} \arcsin y + \alpha_0 y^2: \quad (62)$$

Then the quasiclassical method applied to the Hamiltonian (61) gives

$$\int_{r_0}^{r_+} p_r(r) dr = n + \frac{1}{2} ; \quad (63)$$

with

$$p_r(r) = \frac{q}{\alpha_0 (M - \alpha_0 U(\alpha_0; r)) - m^2}: \quad (64)$$

The eigenvalues $M_{n1}(\alpha_0)$ for $m = 0$ were found numerically from (63), (64) and the minimization procedure with respect to α_0 was used then. Results for M_{n1} are given in Table II and depicted in Fig. 2 demonstrating very nearly straight lines with approximately string slope $(2\pi)^{-1}$ in l and as twice as smaller slope in n . Note that it is the region of intermediate values of r to play the crucial role in the Bohr-Sommerfeld integral (63), i.e.: the region where the nontrivial dependence of the effective potential $U(\alpha_0; r)$ on the angular momentum is most important (see Fig. 1).

In Table III we give comparison of the masses of several light-light mesonic states extracted by means of the numerical results from Table II with the experimental data and theoretical predictions taken from [32]. We have fitted our results to the experimental spectrum using the negative constant M^{-2} (see equation (29)).

C . D iscussion

Let us recall the results obtained for the light-light mesons and discuss problems connected to the given approach. The net result of the current section is the l -dependent effective interquark potential which gives the naive linearly rising interaction only for $l=0$. It was observed long ago [33,2] that for large angular momenta the quark dynamics is negligible and the slope (35) naturally appears from the picture of open rotating string. In the present paper we find that formless quarks even the low-lying mesonic states demonstrate nearly straight-line Regge trajectories with the string slope (35).

One problem clearly seen from our Figs 2,3 is the leading trajectory intercept l_0 ($M^2 = 0$). To reproduce the experimental intercept around -0.5 (see Fig.3) starting from the theoretical one $+0.5$ (see left plot in Fig.2) one needs a large negative constant added either to the Hamiltonian (48) (see e.g. C_0 in equation (54)) or in the form of M^2 directly in (29) (see also Table III). Once the first way might violate the linearity of the Regge trajectories, then one should expect QCD to prefer the second one, though the first way remains more attractive from the practical point of view and will be used in calculations of the heavy-light mesons spectrum in the next section.

Another problem is that one of the most intriguing questions of the mesonic spectroscopy, the splitting (and a similar problem in the strange sector) can not be addressed to our model. Taking the exact solution of the spinless Salpeter equation (11) with $n = l = 0$ (see Table I with an appropriate re-scaling from $= 0.2 \text{ GeV}^2$ to $= 0.17 \text{ GeV}^2$) one finds for the mass squared the value of order 1.7 GeV^2 which does not violate the linearity of the trajectory (see the circled dot in Fig.2). If the overall negative shift with $\frac{q}{j} M^2 j = 1126 M \text{ eV}^2$ (see Table III) is applied to this state, then one arrives at the meson mass about 775 MeV , i.e. the value very close to the experimental one. Note that we have practically coinciding constants for the $-$ and $+$ mesons trajectories (see caption for Table III) that supports the idea that M^2 can be associated with quark selfenergies.

Meanwhile one can not pretend to describe pions (kaons) in the same framework as their

Goldstone nature is not implemented in the current model. In the realistic quantum field theory based models each mesonic state possesses two wave functions which describe forward and backward in time motion of the $q\bar{q}$ pair inside the meson [34]. The backward motion is suppressed if at least one of the quarks is heavy, for highly excited states and in the infinite momentum frame. For the chiral pion, which is expected to be strictly massless in the chiral limit, the two wave functions are of the same order of magnitude (see e.g. [35] for the explicit pionic solution in QCD_2), so that none of them can be neglected. This explains why the naive estimate for the pion mass lies much higher than the experimentally observed value of 140 MeV. For the first excited state, meson, this effect is already suppressed, though one still has to be careful neglecting the backward motion of the quarks. The progress in this direction was achieved in recent papers by one of the authors (Yu.S.) [19], where a Dirac-type equation was derived for the heavy-light system and properties of its solutions were investigated. This new formalism is expected to allow consideration of pionic Regge trajectories as it has the chiral symmetry breaking built-in.

VII. SPECTRUM OF HEAVY-LIGHT MESONS

All results obtained for the light-light mesons in Section V I can be reproduced for the heavy-light states, so that in the one-body limit the Regge trajectories with the correct string (inverse) slope are readily reproduced. Meanwhile the aim of this study is to take into account corrections to the leading regime which come from the spin-dependent terms in the interquark interaction as well as those due to the finiteness of the heavy quark mass. Corrections of both types are important for establishing the correct spectra of D and B mesons which are the main target of the present investigation.

A. Spectrum of the spinless heavy-light system

In this subsection we study the spectrum of the heavy-light mesons disregarding the quark spins. This amounts to solving the Schrodinger-like equation for the Hamiltonian H_0

from (54). Note that to this end one needs to know the non-relativistic spectrum in the potential which is the sum of the linearly rising and the Coulomb parts [26,36,3]:

$$\frac{d^2}{dx^2} + \frac{1}{x} j - \frac{1}{x^2} = a(\rho) ; \quad (65)$$

where

$$= \frac{2}{\rho} = \frac{4}{3} s = \frac{1}{1 + \frac{2}{s}} ;$$

If solutions of (65) for $a(\rho)$ and $a(\rho)$ are known as functions of the reduced Coulomb potential strength s then one can find the following expressions for the extremal values of the einbeins (constituent quark masses):

$$_1(\rho) = \frac{q}{m_1^2 + a^2(\rho)} \quad _2(\rho) = \frac{q}{m_2^2 + a^2(\rho)} \quad (\rho) = \frac{1}{2} \rho - \frac{1}{2} ; \quad (66)$$

with $a(\rho)$ given by

$$^2(\rho) = \frac{1}{3} a + 2 \frac{\partial a}{\partial \rho} ;$$

The definition of the reduced einbein field via $_1$ and $_2$ leads to the equation defining

$$(\rho) = \frac{^1(\rho) _2(\rho)}{^1(\rho) + _2(\rho)} ; \quad (67)$$

Technically this means that one should generate selfconsistent solutions to equations (65) and (67) which are subjects to numerical calculations [36,3]. In Table IV we give such solutions for several radial and orbital excitations in D , D_s , B and B_s mesonic spectra. We use the standard values for the string tension, the strong coupling constant and the current quarks masses. Note that s is chosen close to its frozen value [37] and it does not change a lot between D and B mesons. The reason is that in both cases one has a light quark moving in the field of a very heavy one, so that the one-gluon exchange depends on the size of the system, rather than on its total mass. Once the difference in size between D and B mesons is not that large, the difference between the two values of the strong coupling constant is also small (see Table IV).

The ρ -function at the origin given in the last column of Table IV and which will be used later on for spin-spin splittings is defined for radially excited states as

$$j(0)j^2 = \frac{2}{4} - 1 + h x^2 i ; \quad (68)$$

where

$$h^N i = (2)^{N-3} h x^N i = (2)^{N-3} \sum_{0}^{N-1} x^{N+2} j(x) j^2 ; \quad N > 3 \quad 21; \quad (69)$$

that immediately follows from the properties of equation (65) and the corresponding redefinition of variables.

B. Spin-spin and spin-orbit splittings. The string correction

In this subsection we calculate the spin-dependent corrections to the results given in Table IV as well as those due to the proper string dynamics and which were intensively discussed before.

The eigenstates of the Hamiltonian H_0 from (54), which we consider to be the zeroth approximation, can be specified in the form of terms $s n^{2s+1} L_J$ (n being the radial quantum number) as the angular momentum L , the total spin S , and the total momentum $J = L + S$ are separately conserved by H_0 . The corresponding matrix elements for various operators present in (55) read

$$\begin{aligned} {}^{2s+1}P_J & \\ h^1 P_1 \mathcal{J}_1 L \mathcal{J} P_1 i &= 0 \quad h^1 P_1 \mathcal{J}_2 L \mathcal{J} P_1 i = 0 \quad h^1 P_1 j(S_1 n) (S_2 n) \mathcal{J} P_1 i = \frac{1}{4} \\ h^3 P_0 \mathcal{J}_1 L \mathcal{J} P_0 i &= -1 \quad h^3 P_0 \mathcal{J}_2 L \mathcal{J} P_0 i = -1 \quad h^3 P_0 j(S_1 n) (S_2 n) \mathcal{J} P_0 i = \frac{1}{4} \\ h^3 P_1 \mathcal{J}_1 L \mathcal{J} P_1 i &= \frac{1}{2} \quad h^3 P_1 \mathcal{J}_2 L \mathcal{J} P_1 i = \frac{1}{2} \quad h^3 P_1 j(S_1 n) (S_2 n) \mathcal{J} P_1 i = \frac{1}{4} \\ h^3 P_2 \mathcal{J}_1 L \mathcal{J} P_2 i &= \frac{1}{2} \quad h^3 P_2 \mathcal{J}_2 L \mathcal{J} P_2 i = \frac{1}{2} \quad h^3 P_2 j(S_1 n) (S_2 n) \mathcal{J} P_2 i = \frac{1}{20} \end{aligned} \quad (70)$$

$$^{2S+1}D_J$$

$$h^1 D_2 \mathcal{F}_1 \mathcal{L} \mathcal{J} D_2 i = 0 \quad h^1 D_2 \mathcal{F}_2 \mathcal{L} \mathcal{J} D_2 i = 0 \quad h^1 D_2 j(S_1 n) (S_2 n) \mathcal{J} D_2 i = \frac{1}{4}$$

$$h^3 D_1 \mathcal{F}_1 \mathcal{L} \mathcal{J} D_1 i = \frac{3}{2} \quad h^3 D_1 \mathcal{F}_2 \mathcal{L} \mathcal{J} D_1 i = \frac{3}{2} \quad h^3 D_1 j(S_1 n) (S_2 n) \mathcal{J} D_1 i = \frac{1}{12} \quad (71)$$

$$h^3 D_2 \mathcal{F}_1 \mathcal{L} \mathcal{J} D_2 i = \frac{1}{2} \quad h^3 D_2 \mathcal{F}_2 \mathcal{L} \mathcal{J} D_2 i = \frac{1}{2} \quad h^3 D_2 j(S_1 n) (S_2 n) \mathcal{J} D_2 i = \frac{1}{4}$$

$$h^3 D_3 \mathcal{F}_1 \mathcal{L} \mathcal{J} D_3 i = 1 \quad h^3 D_3 \mathcal{F}_2 \mathcal{L} \mathcal{J} D_3 i = 1 \quad h^3 D_3 j(S_1 n) (S_2 n) \mathcal{J} D_3 i = \frac{1}{28}:$$

The interaction V_{sd} given by (55) mixes orbitally excited states with different spins, so that the transition matrix elements are given by

$$h^1 P_1 \mathcal{F}_1 \mathcal{L} \mathcal{J} P_1 i = \frac{p_1}{2} \quad h^1 P_1 \mathcal{F}_2 \mathcal{L} \mathcal{J} P_1 i = \frac{p_1}{2} \quad (72)$$

$$h^1 D_2 \mathcal{F}_1 \mathcal{L} \mathcal{J} D_2 i = \frac{3}{2} \quad h^1 D_2 \mathcal{F}_2 \mathcal{L} \mathcal{J} D_2 i = \frac{3}{2};$$

which lead to mixing within $\mathcal{J} P_1 i$, $\mathcal{J} P_1 i$, and $\mathcal{J} D_2 i$, $\mathcal{J} D_2 i$ pairs so that the physical states are subject to the matrix equations of the following type:

$$\begin{array}{ccc} E_1 & E & V_{12} \\ & & = 0: \\ V_{12} & E_2 & E \end{array} \quad (73)$$

Another important ingredient is the string correction given by (52) which leads to extra negative shift for orbitally excited states

$$M_1 = \frac{\left(\begin{smallmatrix} 2 & 2 \\ 1 & 2 \end{smallmatrix}\right) \left(\begin{smallmatrix} 1 & 2 \\ 1 & 2 \end{smallmatrix}\right)}{6} 1(1+1)hr^{-1}i: \quad (74)$$

Thus the model is totally fixed and the only remaining fitting parameter is the overall spectrum shift C_0 which finally takes the following values:

$$C_0(D) = 212M \text{ eV} \quad C_0(D_s) = 124M \text{ eV} \quad C_0(B) = 203M \text{ eV} \quad C_0(B_s) = 124M \text{ eV:} \quad (75)$$

Note that C_0 does not depend on the heavy quark ($C_0(D)$, $C_0(B)$, $C_0(D_s)$, $C_0(B_s)$) and is completely defined by the properties of the light one. For states with two light quarks

one would have the overall negative shift $2C_0$ that gives the contribution $4C_0(M_n - C_0)$ into M_n^2 . In case of π meson this provides a negative constant of order 1G eV, i.e: right the value needed to bring the theoretical intercept 1_0 into the correct experimental one (see jM^2j in Table III).

C. Comparison with the experimental and lattice data. "Mystery" of the D (2637) state

In Tables V, VI we compare the results of our numerical calculations for the spectrum and splittings with the experimental and recent lattice data as well as with the theoretical predictions from [32] and [40]. The underlined figures in Table V are considered as the most probable candidates for the experimentally observed values. One can see a good agreement between our theoretical predictions and the experimental values, as well as with the lattice calculations [38,39]. To demonstrate the relevance of the corrections due to the heavy mass we consider a simplified system containing one infinitely heavy particle and the light one having its real mass. The best fits for the experimental spectra with the results for such simplified systems are also given in Table V in the column entitled $M_{h1}^{(0)}$ for comparison. One can easily see that corrections in the inverse powers of the heavy mass are strongly needed to reproduce the experimental spectrum with a reasonable accuracy and to remove degeneracy of S-states.

Now we are in the position to resolve the "mystery" of the D (2637) state (and a similar one in the B mesons spectrum). This state was claimed recently by DELPHI Collaboration [4,5], but once its quantum numbers were not defined, then there was a problem of the identification of this state. In most quark models (see also Table V) the first radial excitation $J^P = 0^-$ lies approximately in the desired region of mass, but estimates of the width of such a state lead to a confusion, as all such estimates give values much larger than the width of about 15M eV reported by DELPHI. The only would-be way out of the problem is to identify this narrow state with orbital excitations with J^P being 2 or 3. In spite of the

fact that orbitally excited states are really narrower than the radially excited ones and they can have the width compatible with the experimental value, the following two objections can be made [41]: i) quark models predict orbitally excited mesons to be at least 50 MeV heavier than needed, ii) a neighboring slightly more massive state should be observed as well.

It follows from Table V that we can remove both objections mentioned above (see also [3]). Indeed, one can easily see that orbitally excited states 2 and 3 lie even somewhat lower than the radial excitation 0. The reason for that is the negative string correction (74) for the orbitally excited states which comes from the proper dynamics of the string. Besides that, the single D-wave 3 state is even more probable candidate for the role of the observed D (2637) resonance than the lightest one from the pair of states 2, so that the problem of the "missing state" is also avoided.

Note that our predictions D (2654), D (2663) and D (2664) give larger masses compared to the experimental one. This must be a reflection of the general lack of the variational einbein field method (-technique) discussed before, which gives slightly overestimated values for the spectrum of excited states (see Table I and discussion in subsection III D).

D . A bridge to the Heavy Quark Effective Theory

In this subsection we discuss the correspondence between our model and the Heavy Quark Effective Theory (HQET) approach widely discussed in literature (see [42,43] and references therein). We use the standard parametrization for the heavy-light meson mass

$$M_{hl} = m_Q + \frac{1}{2m_Q} (1 + d_H) + O \left(\frac{1}{m_Q^2} \right); \quad (76)$$

where m_Q is the mass of the heavy constituent, coefficient d_H describes the hyperfine splitting

$$d_H = \begin{cases} \frac{8}{3} & \text{for 0 states} \\ \frac{1}{3} & \text{for 1 states;} \end{cases} \quad (77)$$

whereas α_1 and α_2 are the free parameters which are the subject to theoretical investigation. Parameter α_2 is directly connected to the splitting between 1^3S_1 and 1^1S_0 states and can be estimated from the experimental mesonic spectrum to be

$$\alpha_2 = \frac{1}{4} (M_B - M_{B_0}) / 0.12 \text{ GeV}^2 : \quad (78)$$

From Table V I one can easily find our prediction for α_2

$$\alpha_2 = 0.16 \text{ GeV}^2 ; \quad (79)$$

which being slightly overestimated is still in a reasonable agreement with the experimental value (78).

In the meantime our model allows direct calculation of the parameters α_1 and α_2 based on the Hamiltonian (54). We apply the variational procedure described above to the idealized system with $m_1 = m_Q = 1$ and $m_2 = 0$. This yields

$$= \frac{p^2}{4} - \frac{2}{3} a(0) + \frac{V_0}{12} a(0) + 2 \frac{\partial a}{\partial r} \Big|_0^5 ; \quad (80)$$

where $\alpha = \frac{4}{3} s$, $a(\cdot)$ is the dimensionless eigenvalue introduced in (65) (see subsection V IIA); a_0 is solution to the equation

$$\alpha_2 = \frac{4}{3} a^2 + 2 \frac{\partial a}{\partial r} \Big|_0^5 ; \quad (81)$$

Then one can extract the coefficient α_2 from the first term in equation (55):

$$\alpha_2 = \frac{4}{3} j(0) \Big|_0^2 = \frac{2}{3} \left(1 + a_0 \right) : \quad (82)$$

The analytical formula for a_0 is also available, but it is rather bulky and we do not give it here. For $s = 0.39$ one can find the numerical solution to equation (81) to be $a_0 = 1.175$. The corresponding values for α_1 and α_2 are given in the first column of Table V II where they are compared with the results of other approaches.

Another way to estimate the discussed constants is to find the best t of the form

$$M_{\text{fit}} = m_Q + t + C_0 \frac{1}{2m_Q} \quad (83)$$

with α_1 and α_2 being the fitting parameters and $C_0 = 203 \text{ eV}$ taken from (75), for the eigenvalues of the Hamiltonian (54) with m_Q varied around the bottom quark mass $m_b = 4.8 \text{ GeV}$ (we use the region $4 \text{ GeV} < m_Q < 6 \text{ GeV}$). The coefficient α_2 can be found using formula (82) with α_0 changed for the exact solution for α taken from Table IV. Results are listed in the second column of Table V II.

One can see our figures to be in general agreement with those found in other approaches among which we mention the QCD sum rules method [44], the inclusive semileptonic B mesons decays [45] and the Dyson-Schwinger equation for the system of the light quark and the static antiquark [46]. We find parameter α_1 to be rather sensitive to the strong coupling constant α_s . For example for $\alpha_s = 0.3$ one has $\alpha_1 = 0.38 \text{ GeV}^2$ which should be confronted with the value $\alpha_1 = 0.506 \text{ GeV}^2$ from the first column of the Table V II found for $\alpha_s = 0.39$.

All our predictions for α_2 exceed the value given by equation (78). The reason is slightly overestimated value of $\alpha(0)$ given by the variational einbein field approach.

One should appreciate the advantage of the einbein field method which allows to obtain relatively simple analytical formulae for various parameters and to investigate their dependence on the strong coupling constant α_s (dependence on the only dimensional parameter is uniquely restored giving $\alpha = \alpha_s^p$ and $\alpha_1 = \alpha_2 = 0$).

V III. CONCLUSIONS

In conclusion let us briefly recall the main results obtained in the present paper.

We use the model for the QCD string with quarks at the ends to calculate the spectra of light-light and heavy-light mesons. There are two main points in which we differ from other approaches to the same problem based on various relativistic Hamiltonians and equations with local potentials. The first point is that we do not introduce the constituent mass by hands. On the contrary, starting from the current mass we naturally arrive at the effective quark masses which appear due to the interaction. Moreover, the resulting effective mass is large enough even for the lightest quarks and lowest states in the spectrum, so that the

spin-dependent terms in the interquark interaction can be treated as perturbations in most cases (except for pions and kaons) and thus accounted for in this way.

The second advantage of the method is that the dynamics of the QCD string naturally enters the game and it can be studied systematically. The proper account for this dynamics allows to resolve several problems of the mesonic spectroscopy, namely one can find that the rotating string lowers down the masses of orbitally excited states bringing the (inverse) slope of Regge trajectories into their correct values (2 for light-light and for heavy-light states). Besides, this allows to resolve the problem of the identification of the D (2637) state recently claimed by DELPHIC collaboration and which is known to lead to a contradiction between its small width, incompatible with the decay modes for the radial excitation, and its mass lying considerably lower than the values predicted by the quark models for orbitally excited states. In the meantime taking into account the negative string correction contributing into the masses of orbitally excited mesons readily resolves this "mystery" for D (2637) state as well as for its counterpart in the spectrum of B mesons.

For heavy-light system we extract the constants α_1 and α_2 used in the framework of the Heavy Quark Effective Theory, for which we derive analytical formulae. We find our numerical results to be in agreement with those obtained from the experimental data and calculations in other approaches like QCD sum rules, inclusive semileptonic B mesons decays and relativistic Dyson-Schwinger equation for the qQ system.

We also conclude that the string-like interaction favoured by QCD invalidates the very notion of any local interquark potential still leaving room to the einbein field method for the Hamiltonian approach to the bound states of quarks and gluons in QCD. Being rather accurate, this method still requires improvements to increase the accuracy and to have the full control over it.

The authors are grateful to A M Badalian, P Bicudo, R N Faustov, A B Kaidalov, V S Popov and E Ribeiro for useful discussions and valuable comments and to V L M organov and B L G Bakker for providing numerical solutions to some equations. One of the authors

(A.N.) would like to thank the staff of the Centro de Física das Interacções Fundamentais (CFF-IST) for cordial hospitality during his stay in Lisbon.

Financial support of RFFI grants 00-02-17836 and 00-15-96786, INTAS-RFFI grant IR-97-232 and INTAS CALL 2000, project # 110 is gratefully acknowledged.

- [1] J.M. erlin and J.P. aton, J. Phys. G 11 (1985) 439
- [2] A.Yu. Dubin, A.B. Kaidalov, Yu.A. Simonov, Phys. Lett. B 323 (1994) 41; Phys. Lett. B 343 (1995) 310
- [3] Yu.S. Kalashnikova and A.V. Nefediev, Phys. Lett. B 492 (2000) 91
- [4] DELPHI Collaboration, P. Abreu et al., Phys. Lett. B 426 (1998) 231
- [5] M. Feindt, O. Podorin (DELPHI Collaboration), contrpa01-021 ICHEP '96 Warshaw, DELPHI 96-93 CONF 22;
C. Wieser, Proceedings of the 28th International Conference on High Energy Physics, editors Z. Ajduk, A.K. Wobblewski, World Scientific, Singapore 1997), page 531
- [6] Yu.S. Kalashnikova and A.V. Nefediev, Phys. Atom. Nucl. 60 (1997) 1389
- [7] L. Brink, P.D. iVecchia, P. Howe, Nucl. Phys. B 118 (1977) 76
- [8] E.S. Fradkin and D.M. Gitman, Phys. Rev. D 44 (1991) 3230;
G.V. Gregoryan and R.P. Gregoryan, Phys. Atom. Nucl. 53 (1991) 1737;
Yu.S. Kalashnikova and A.V. Nefediev, Phys. Atom. Nucl. 62 (1999) 377
- [9] A.M. Polyakov, "Gauge Fields and Strings", Harwood Academic Publishers, 1987;
- [10] F. Rohrlich, Ann. Phys. 117 (1979), 292
M. J. King, F. Rohrlich, Ann. Phys. 130 (1980), 350
- [11] P.A.M. Dirac, "Lectures on Quantum Mechanics", Belfer Graduate School of Science, Yeshiva

University, New York (1964)

[12] Yu S K alashnikova and A V Nefediev, PhysLett. B 399 (1997) 274; PhysAtom Nucl. 61 (1998) 785

[13] Yu A S im onov, PhysLett. B 226 (1989) 151

[14] Yu A S im onov, in Proceedings of Hadron'93 (Com o, 21-25 June 1993), ed. T B ressani, A Felicielo, G P reparata and P G R atcli e; Yu S K alashnikova and Yu B Yufryakov, Phys. Lett. B 359 (1995) 175; Yad F iz. 60 (1997) 374

[15] Yu A S im onov and A B K aidalov, PhysLett. B 477 (2000) 163; PhysAtom Nucl. 63 (2000) 1428

[16] V D M ur, B M K amakov and V S Popov, in preparation, to be submitted to ZhETP

[17] V D M ur, V S Popov, Yu A S im onov and V P Yurov, JETP 75 (1994) 1

[18] M S M arinov and V S Popov, JETP 67 (1974) 1250
V L E ketsky, V D M ur, P S Popov and D N V oskresensky, JETP 76 (1979) 431;
PhysLett. B 80 (1978) 68

[19] Yu A S im onov, Yad. F iz. 60 (1997) 2252, hep-ph/9704301;
Yu A S im onov, JA T jpn, PhysRev. D 62 (2000) 094511

[20] V L M orgunov, A V Nefediev and Yu A S im onov, PhysLett. B 459 (1999) 653

[21] V L M orgunov, V I. Shevchenko, Yu A . S im onov, PhysAtom Nucl. 61 (1998) 664

[22] G F Chew, Rev Mod Phys. 34 (1962) 394

I.Yu K obzarev, B V . M artem yanov, M G Schepkin, UFN 162 (1992) 1 (in Russian)

M G O lsson PhysRevD 55 (1997) 5479

B M B arbashov and V V N esterenko, Relativistic string model in hadron physics, Energoatomizdat, M oscow , 1987 (in Russian)

[23] T J A llen, M G O lsson, S Veseli, PhysRev. D 62 (2000) 094021

[24] Yu A Simonov, NuclPhys. B 307 (1988) 512;
 Yu A Simonov and J.A. Tjon, Ann Phys. (N.Y.) 228 (1993) 1

[25] H.G. Dosch, PhysLett. B 190 (1987) 177;
 H.G. Dosch and Yu A Simonov, PhysLett. B 205 (1988) 339;
 Yu A Simonov, NuclPhys. B 307 (1989) 67

[26] Yu A Simonov, in Proceedings of the XVII International School of Physics "QCD: Perturbative or Nonperturbative", Lisbon, 29 September - 4 October 1999, Editors L.S. Ferreira, P. Nogueira and J.I. Silva-Marcos (World Scientific 2000), page 60

[27] A.M. Badalian, Yu A Simonov, Yad. Fiz. 59 (1996) 2247

[28] E. Eichten and F.L. Feinberg, PhysRev. D 23 (1981) 2724;
 D. Gross, Z. Phys. C 26 (1984) 401

[29] A.M. Badalian and B.L.G. Bakker in preparation

[30] J. Pantaleone, S.-H. Henry Tye, Y. J. Ng, PhysRev. D 33 (1986) 777

[31] Yu A Simonov, NuclPhys. B 592 (2000) 350

[32] S. Godfrey, N. Isgur, PhysRev. D 32 (1985) 189; S. Godfrey, R. Kokoski, PhysRev. D 43 (1991) 1679

[33] Dan La Course and M. G. Olsson, PhysRev. D 39 (1989) 1751;
 C. Olsson and M. G. Olsson, MAP/PH/76/ (1993)

[34] A. Le Yaouanc, L. Oliver, O. Pene and J.-C. Raynal, Phys. Rev. D 29, 1233 (1984);
 A. Le Yaouanc, L. Oliver, S. Ono, O. Pene and J.-C. Raynal, Phys. Rev. D 31 137 (1985);
 P. Bicudo and J.E. Ribeiro, Phys. Rev. D 42, 1611 (1990);
 I. Bars and M. B. Green, Phys. Rev. D 17, 537 (1978)

[35] Yu S. Kalashnikova, A. V. Nevediev and A. V. Volodin, Phys. At. Nucl. 63 (2000) 1623;
 Yu S. Kalashnikova and A. V. Nevediev, PhysLett. B 487 (2000) 371

[36] Yu A Simonov, *Z Phys. C* 53 (1992) 419

[37] Yu A Simonov, *Yad Fiz.* 58 (1995) 113; *JETP Lett.* 57 (1993) 513

[38] J. Hein et.al., *Phys. Rev. D* 62 (2000) 074503

[39] R Lewis, R M Woloshyn, *Phys. Rev. D* 62 (2000) 114507

[40] D Ebert, V O Galkin, R N Faustov, *Phys. Rev. D* 57 (1998) 5663

[41] D Melikhov and O Pene, *Phys. Lett. B* 446 (1999) 336;
P R Page, *Phys. Rev. D* 60 (1999) 057501

[42] N Isgur, M Wise, *Phys. Lett. B* 234 (1989) 113; *B* 237 (1990) 527

[43] T Mannel, in *Lecture Notes in Physics*, Springer, v.479, p.139, 1996

[44] P Ball and V Braun, *Phys. Rev. D* 49 (1994) 2472

[45] M Gremm, A Kapustin, Z Ligeti, M B Wise, *Phys. Lett. B* 377 (1996) 20

[46] Yu A Simonov, J A Tjon, *Phys. Rev. D* 62 (2000) 014501

n	0	1	2	3	4	5
M_n (WKB)	1.373	2.097	2.629	3.070	3.455	3.802
M_n (einbein)	1.483	2.256	2.826	3.300	3.713	4.085
M_n (combined)	1.475	2.254	2.825	3.299	3.713	4.085
M_n (exact)	1.412	2.106	2.634	3.073	3.457	3.803
$\frac{M_n \text{ (combined)} - M_n \text{ (exact)}}{M_n \text{ (combined)}}, \%$	4.27	6.57	6.76	6.85	6.89	6.90

TABLE I. Comparison of the numerical results of the three approximate methods of solving the eigenvalues problem for equation (11) for $m = 0$, $\epsilon = 0.2 \text{ GeV}^2$ and $l = 0$ given by equations (23)–(25) with the exact eigenenergies of the Hamiltonian H_1 from (22).

n l	1	2	3	4	5
0	1.719	2.029	2.287	2.516	2.725
1	2.362	2.611	2.829	3.025	3.208
2	2.850	3.069	3.264	3.442	3.608
3	3.259	3.460	3.639	3.803	3.955
4	3.619	3.806	3.973	4.127	4.268
5	3.944	4.120	4.276	4.423	4.554

TABLE II. Quasiclassical spectrum of Hamiltonian (61), (62) for $m = 0$ and $\epsilon = 0.17 \text{ GeV}^2$ minimized with respect to the einbein e_0 (combined method).

Meson	$2S+1L_J$	$J^P C$	$M_{\text{exp}}; M \text{ eV}$	$M_{\text{theor}}; M \text{ eV}$	$M_{\text{theor}} [32]; M \text{ eV}$	Error; %
	3S_1	1	770	775	770	0.6
3	3D_3	3	1690	1688	1680	0.1
5	3G_5	5	2330	2250	2300	3.4
a_1	3P_1	1^{++}	1260	1346	1240	6.8
a_3	3F_3	3^{++}	2070	2021	2050	2.4
a_2	3P_2	2^{++}	1320	1316	1310	0.5
a_4	3F_4	4^{++}	2040	2002	2010	1.9
a_6	3H_6	6^{++}	2450	2491	-	1.7

TABLE III. Comparison of the masses of the light-light mesons lying on the lowest Regge trajectories ($n = 0, S = 1, J = 1+1$ for a_1 and a_2 trajectories; $n = 0, S = 1, J = 1$ for a_1 trajectory), calculated for $\alpha = 0.17 \text{ GeV}^2$ and the overall negative shifts $\frac{P}{j M^2} = 1126 \text{ MeV}$ for the a_1 trajectory, $\frac{P}{j M^2} = 1070 \text{ MeV}$ for a_1 trajectory and $\frac{P}{j M^2} = 1105 \text{ MeV}$ for the a_2 trajectory, with the experimental data and with the theoretical predictions taken from [32]. See also discussion concerning the pion and the meson masses in subsection V IC.

n	l	meson	m_1	m_2	s	1	2	E_0	$j(0)$
0	0	D	1.4	0.009	0.17	0.4	0.817	1.497	0.529
		D_s	1.4	0.17	0.17	0.4	0.847	1.501	0.569
		B	4.8	0.005	0.17	0.39	0.999	4.840	0.619
		B_s	4.8	0.17	0.17	0.39	1.035	4.842	0.658
0	1	D	1.4	0.009	0.17	0.4	0.869	1.522	0.597
		D_s	1.4	0.17	0.17	0.4	0.891	1.525	0.629
		B	4.8	0.005	0.17	0.39	1.052	4.847	0.675
		B_s	4.8	0.17	0.17	0.39	1.080	4.849	0.707
0	2	D	1.4	0.009	0.17	0.4	0.924	1.554	0.674
		D_s	1.4	0.17	0.17	0.4	0.942	1.557	0.702
		B	4.8	0.005	0.17	0.39	1.128	4.860	0.762
		B_s	4.8	0.17	0.17	0.39	1.151	4.861	0.789
1	0	D	1.4	0.009	0.17	0.4	0.929	1.557	0.682
		D_s	1.4	0.17	0.17	0.4	0.947	1.561	0.710
		B	4.8	0.005	0.17	0.39	1.142	4.863	0.779
		B_s	4.8	0.17	0.17	0.39	1.165	4.864	0.806

TABLE IV. Solutions of the equations (65)–(67) for standard values of the string tension α_s , the strong coupling constant α_s and the current masses of the quarks. E_0 is the mass of the corresponding state. All parameters are given in GeV to the appropriate powers.

	$n^{2s+1}L_J$	J^P	M _{exp}	M _{theor}	M _{hl} ⁽⁰⁾	M _{theor} [32]	M _{theor} [40]	M _{lat} [38]	M _{lat} [39]
D	1^1S_0	0	1869	1876	2000	1880	1875	1884	1857
D	1^3S_1	1	2010	2022	2000	2040	2009	1994	1974
D ₁	$1^1P_1 = ^3P_1$	1^+	2420	2354 2403	2393 2407	2440=2490	2414=2501		2405=2414
	1^3P_0	0^+		2280	2400	2400	2438		2444
D ₂	1^3P_2	2^+	2460	2432	2400	2500	2459		2445
D ₀	1^3D_3	3	2637	2654	2600	2830			
	$1^1D_2 = ^3D_2$	2		2663	2573				
				2729	2600				
	2^3S_1	0		2664	2500	2640	2629		
D _s	1^1S_0	0	1968	1990	2100	1980	1981	1984	input
D _s	1^3S_1	1	2112	2137	2100	2130	2111	2087	2072
D _{1s}	$1^1P_1 = ^3P_1$	1^+	2536	2471 2516	2494 2506	2530=2570	2515=2569	2494	2500=2511
	1^3P_0	0^+		2395	2500	2480	2508		2499
D _{2s}	1^3P_2	2^+	2573	2547	2500	2590	2560	2411	2554
B	1^1S_0	0	5279	5277	5200	5310	5285	5293	5277
B	1^3S_1	1	5325	5340	5200	5370	5324	5322	5302
B ₁	$1^1P_1 = ^3P_1$	1^+	5732	5685 5719	5592 5608		5719=5757		5684=5730
	1^3P_0	0^+		5655	5600	5760	5738		5754
B ₂	1^3P_2	2^+	5731	5820	5600	5800	5733		5770
B ₀	1^3D_3	3	5860	5955	5800	6110			
	$1^1D_2 = ^3D_2$	2		5953	5773				
				6018	5827				

	2^3S_1	0		5940	5700	5930	5898	5890	
B_s	1^1S_0	0	5369	5377	5400	5390	5375	5383	input
B_s	1^3S_1	1	5416	5442	5400	5450	5412	5401	5395
B_{1s}	$1^1P_1=^3P_1$	1^+	5853	5789 5819	5793 5807	5860=5860	5831=5859	5783	5794=5818
	1^3P_0	0^+		5757	5800	5830	5841		5820
B_{2s}	1^3P_2	2^+		5834	5800	5880	5844	5848	5847

TABLE V. Masses of the D , D_s , B and B_s mesons in MeV. For the lattice results we give only the central values extracted from Figures 26,27 and Tables XXVIII, XXIX of [38] and from Table V III of [39]. We also compare our results with theoretical predictions taken from [32] and [40]. Symbols $1^1P_1=^3P_1$ and $1^1D_2=^3D_2$ are used to indicate that the physical states are mixtures of the 1^1P_1 and 1^3P_1 or 1^1D_2 and 1^3D_2 states respectively. Underlined figures give masses of the most probable candidates for the experimentally observed resonances. The column $M_{h1}^{(0)}$ contains the best fit to the experimental spectrum for the system containing one particle being ininitely heavy.

Splitting	$D_s\{D$	$D_s\{D$	$D\{D$	$D_s\{D_s$	$B_s\{B$	$B_s\{B$	$B\{B$	$B_s\{B_s$
Experiment	99	102	141	144	90	91	46	47
Theory	114	115	146	147	100	102	63	65
Theory [32]	100	90	160	150	80	80	60	60
Lattice [38]	100	92	110	103	90	90	30	29
Lattice [39]	112	98	117	103	92	93	25	29

TABLE VI. Splittings for the D , D_s , B and B_s mesons in MeV. Lattice results are taken from Tables XXVIII, XXIX of [38] and Table V III of [39]. We give also results of the theoretical papers [32].

	$m_1 \neq 1, m_2 \neq 0$	B mesons	Sum rules [44]	B mesons decays [45]	DS equation [46] ⁵
α_s, GeV	0.471	0.485	0.4 0.5	0.39 0.11	0.493/0.288
α_s, GeV^2	-0.506	-0.379	-0.52 0.12	-0.19 0.10	-
α_s, GeV^2	0.21	0.17	0.12	0.12	-

TABLE VII. Standard parameters used in HQET (see equation (76)). In the first column we give the values following from the formulae (80) and (82) for m_1 and m_2 and the corresponding one for m_Q , the second column contains the best fit of the form $m_Q + \alpha_s + C_0 - \frac{1}{2m_Q}$ for the eigenvalues of the Hamiltonian (54) for m_Q in the region $4\text{GeV} < m_Q < 6\text{GeV}$ (around $m_b = 4.8\text{GeV}$), $C_0 = 203\text{MeV}$ being the overall negative shift constant taken from equation (75). The two numbers given in the last column correspond to local/nonlocal kernels of the Dyson-Schwinger (DS) equation (see [46] for details). The figures given in the first two columns correspond to $\alpha_s = 0.17\text{GeV}^2$ and $\alpha_s = 0.39$.

⁵Note that slightly different values for the string tension ($\alpha_s = 0.18\text{GeV}^2$) and the strong coupling constant ($\alpha_s = 0.3$) were used in this paper.

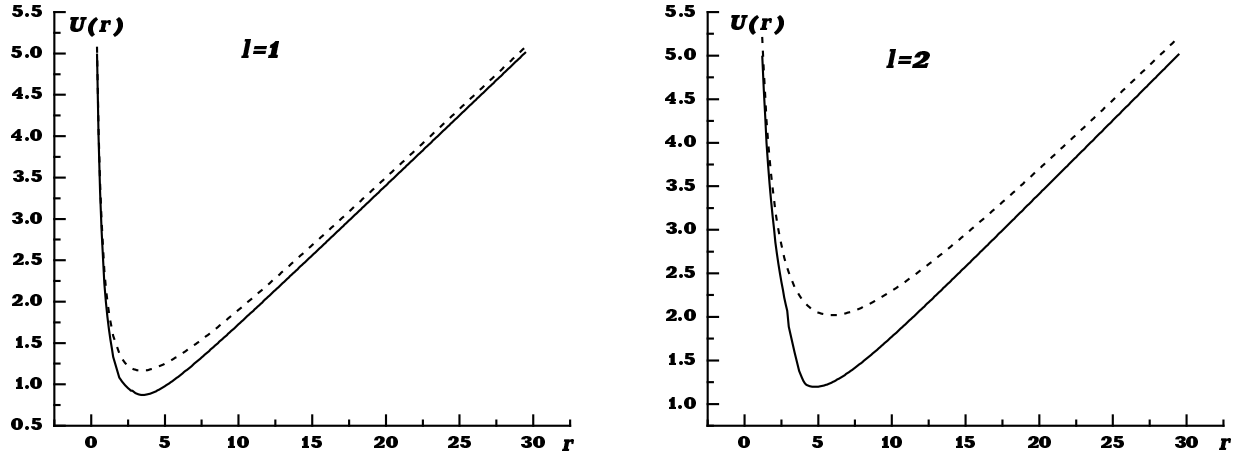


FIG. 1. Effective potential incorporating the string rotation as well as the quark radial motion for $\alpha = 0.17 \text{ GeV}^2$ and two values of the angular momentum l (solid line). The naive sum of the quark centrifugal barrier for the given l and the linearly rising potential $\propto r$ is given in each graph by the dotted line. For $l=0$ the effective potential coincides with $\propto r$ for all values of r .

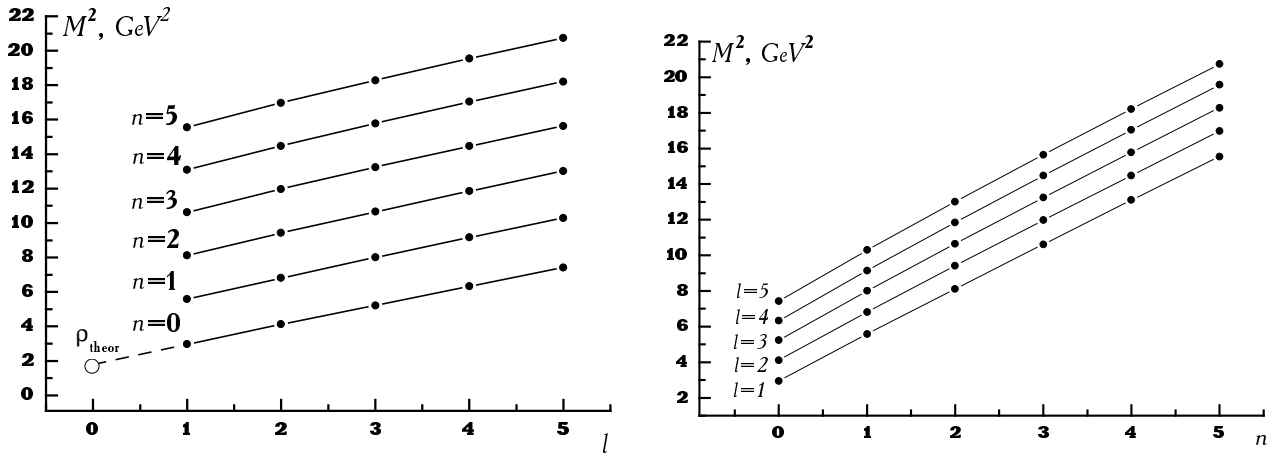


FIG. 2. The Regge trajectories for the Hamiltonian (56) for $m = 0$ and $\alpha = 0.17 \text{ GeV}^2$ (see Table II). Theoretical prediction for the π meson mass $M^2 = 1.7 \text{ GeV}^2$, see figures in Table I for $n = 0$) is shown not to violate the straight-line behaviour of the leading theoretical trajectory (see left plot).

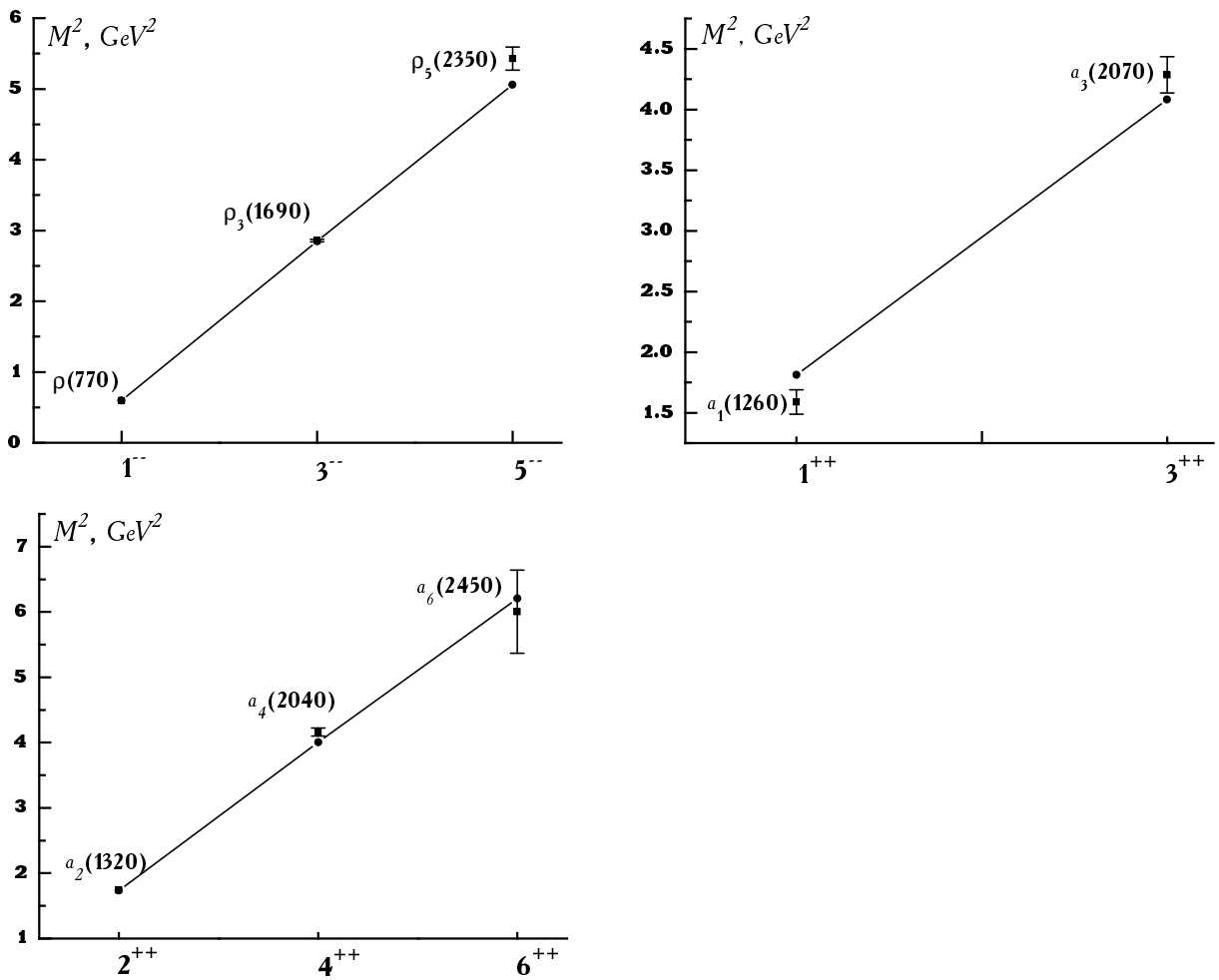


FIG. 3. The lowest Regge trajectories for light-light mesons fitted with respect to the overall negative mass shift (see Table III). The theoretical values for $m = 0$ and $\omega = 0.17 \text{ GeV}^2$ are marked with dots, the experimental data are given by boxes with error bars.